All-Spin-Orbit Switching of Perpendicular Magnetization

Mohammad Kazemi, *Student Member, IEEE*, Graham E. Rowlands, Shengjie Shi, Robert A. Buhrman, and Eby G. Friedman, *Fellow, IEEE*

***Abstract*— Devices with ferromagnetic layers possessing a perpendicular magnetic easy axis are of great interest due to miniaturization capability and thermal stability, retaining deeply scaled magnetic bits over long periods of time. While the tunneling magnetoresistance effect has significantly enhanced electrical reading of magnetic bits, fast and energy efficient writing of magnetic bits remains a challenge. Current-induced spin-orbit torques (SOTs) have been widely considered due to significant potential for fast and energy-efficient writing of magnetic bits. However, to deterministically switch the magnetization of a perpendicularly magnetized device using SOTs, the presence of a magnetic field is required, which offsets possible advantages and hampers applications. In this paper, a perpendicularly magnetized device is presented, which, without the need for a magnetic field, can be deterministically switched in both toggle and nontoggle modes using a damping-like SOT induced by an in-plane current pulse. This capability is realized by shaping the magnetic energy landscape. Present device does not require any materials other than those widely utilized in conventional spin-orbit devices. The device provides two orders of magnitude enhancement in switching energy-time product as compared with state-of-the-art perpendicularly magnetized devices operating on spin-transfer torques.**

***Index Terms*— Magnetic energy landscape, magnetic random access memory (MRAM), magnetic tunnel junction (MTJ), perpendicular magnetic anisotropy (PMA), spin-orbit torques (SOTs).**

I. Introduction

COUPLING between electron spin and orbital motion can be exploited to induce nonequilibrium spin accumulation, which exerts torques, referred to as spin-orbit torques (SOTs), on the magnetization [1], [2]. Heterostructures comprising a ferromagnetic (F) layer sandwiched between an insulating (I) layer and a nonmagnetic heavy metal (NM) layer with strong spin-orbit coupling exhibit SOTs [3]–[15]. Injecting a current pulse into the plane of an $NM|F|I$ heterostructure gives rise to spin accumulation, which produces effective SOTs [4], [5], namely, a field-like torque, $\mathbf{T}_{\mathrm{FL}} = \mathbf{T}_{\mathrm{FL}}^{0}\ \mathbf{m} \times \boldsymbol{\delta}$, and a damping-like torque, $\mathbf{T}_{\mathrm{DL}} = \mathbf{T}_{\mathrm{DL}}^{0}\ \mathbf{m} \times (\boldsymbol{\delta} \times \mathbf{m})$. Here, $\mathbf{T}_{\mathrm{DL}}^{0}$ and $\mathbf{T}_{\mathrm{FL}}^{0}$ each represents a current-dependent proportionality factor and $\mathbf{m}(\boldsymbol{\delta})$ is a unit vector that denotes the direction of the magnetization (the direction traverse to the current flow). Several studies have demonstrated that $\mathbf{T}_{\mathrm{DL}}$ is sufficiently strong to switch the magnetization of a heterostructure with perpendicular [3], [5], [6] or in-plane [15] anisotropy for current densities of the order of 10^7–10^9 A/cm^2.

Perpendicularly magnetized devices have been widely considered due to miniaturization capability and thermal stability, retaining deeply scaled magnetic bits over long periods of time [16]. To date, however, symmetric effects in current-induced SOTs on perpendicular magnetization have prevented SOTs to deterministically switch the magnetization of perpendicularly magnetized devices. Independent of the direction of an in-plane current pulse injected into the device, SOTs equally favor the stable states of perpendicular magnetization, moving the magnetization direction from a perpendicular-to-the-plane stable state into an in-plane metastable state. Once the current is turned off, the SOTs vanish and the magnetization randomly moves from the metastable state to either of the stable states, as determined by the thermal noise. Consequently, the presence of a magnetic field is necessary to permit each current direction to favor a particular stable state of magnetization, allowing the switching operation via SOTs to be deterministic [4], [5].

A magnetic field may be achieved by integrating a permanent magnet within a device. The presence of a magnetic field is, however, undesirable for practical reasons. A magnetic field reduces the energy barrier between the stable magnetization states, thereby lowering the thermal stability of the device. Some recent studies [17], [18] have proposed switching in tapered $NM|F|I$ heterostructures, where the thickness of the I or F layer is reduced toward one end to, respectively, introduce additional torque components [17] or tilt the magnetic anisotropy from the perpendicular direction [18]. Tapered devices are, however, undesirable from a technological point of view. A complex fabrication process is required to accurately control the continuously varying thickness of the I or F layer in tapered devices. Furthermore, tilting magnetic anisotropy from the perpendicular direction emulates the effect of a magnetic field, compromising the thermal stability and restricting device scaling.

In this paper, a perpendicularly magnetized device is introduced, which, without the need for a magnetic field, can be deterministically switched in both toggle and nontoggle

Manuscript received June 19, 2016; revised July 31, 2016; accepted August 14, 2016. Date of publication October 4, 2016; date of current version October 20, 2016. The research is based upon work supported in part by the IARPA, via contract W911NF-14-C0089. The review of this paper was arranged by Editor G. L. Snider.

M. Kazemi and E. G. Friedman are with the Department of Electrical and Computer Engineering, University of Rochester, Rochester, NY 14627 USA (e-mail: mkazemi@ece.rochester.edu; friedman@ece.rochester.edu).

G. E. Rowlands is with the Raytheon BBN Technologies, Cambridge, MA 02138 USA (e-mail: graham.rowlands@bbn.com).

S. Shi and R. A. Buhrman are with the School of Applied and Engineering Physics, Cornell University, Ithaca, NY 14853 USA (e-mail: ss2882@cornell.edu; rab8@cornell.edu).

Color versions of one or more of the figures in this paper are available online at http://ieeexplore.ieee.org.

Digital Object Identifier 10.1109/TED.2016.2604215

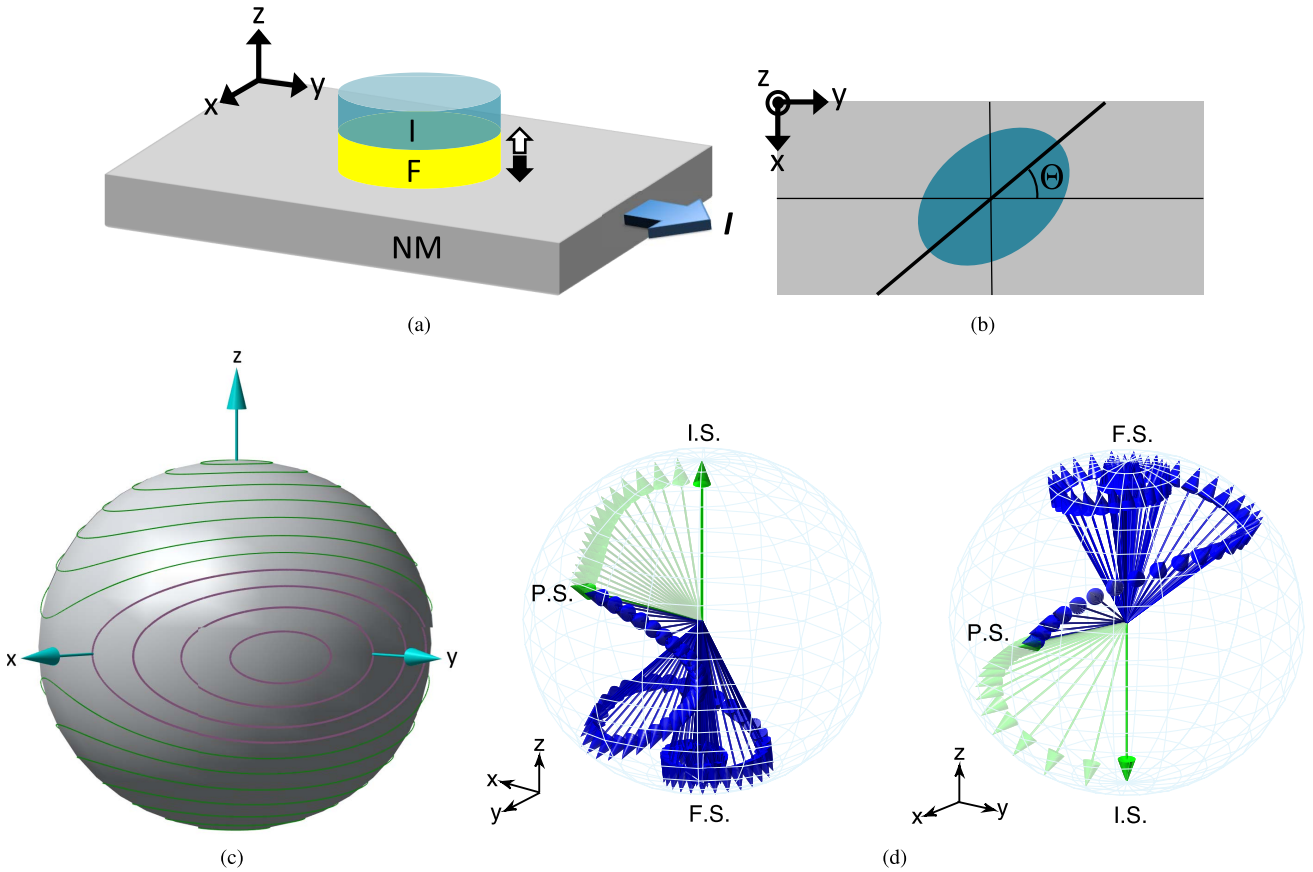

Fig. 1. Structure and operation of the ALPE device. (a) Device structure. The device is composed of a ferromagnetic (F) layer sandwiched between an insulating (I) layer and a nonmagnetic heavy metal (NM) layer with strong spin-orbit coupling. The NM, F, and I layers are all uniformly thick. The stable states of magnetization are illustrated with black and white arrows along the $+z$- and $-z$-directions. To switch the magnetization, a current pulse (I) is injected along the y-axis into the device. (b) x–y cross section of the device. The length of the elliptic cross section encloses an angle of Θ degrees with the $+y$-direction. (c) Energy landscape of the device. Certain energy contours cross the device plane ($x-y$ plane), allowing the damping-like SOT ($\mathbf{T}_{\mathrm{DL}}$) to switch the perpendicular magnetization without the need for a magnetic field. Due to the azimuthal rotation of the $F|I$ pillar by an angle of Θ with respect to the $+y$-direction, the axis passing through the center of the x–y crossing energy contours encloses an angle of Θ degrees with the $+x$-direction. The magnetic energy landscape is, therefore, asymmetric with respect to the current flow and $\mathbf{T}_{\mathrm{DL}}$. (d) Switching the magnetization, by injecting a current pulse, from the $+z$- to $-z$-direction (left) and from the $-z$- to $+z$-direction (right). IS, PS, and FS represent the magnetization state, respectively, when the current pulse is turned on, when the current pulse is turned off, and after the current pulse is injected.

modes using a damping-like SOT induced by an in-plane current pulse. The proposed device, referred to as the all-spin-orbit perpendicularly magnetized (ALPE) device, is composed of layers with a uniform thickness, and does not require any material other than those materials widely utilized in conventional spin-orbit devices. Hence, the device is compatible with existing magnetic recording technology, enhancing the ease of fabrication of the device. In this paper, the magnetic energy landscape of nanomagnets is demonstrated to be the key to deterministic switching of perpendicular magnetization using SOTs in the absence of a magnetic field. The ALPE device achieves all-spin-orbit switching of perpendicular magnetization in both toggle and nontoggle modes by choosing the appropriate amplitude or duration of an injected current pulse. The operation of the ALPE device is demonstrated through macrospin and micromagnetic simulations at room temperature. The ALPE device provides two orders of magnitude enhancement in switching time-energy product as compared with state-of-the-art perpendicularly magnetized devices operating on spin-transfer torques.

The rest of this paper is organized as follows. The structure of the device is explained in Section II. Operation of the device is discussed in Section III. The paper is concluded in Section IV.

II. Structure of the ALPE Device

The basic concept underlying the ALPE device is shown in Fig. 1. The device is composed of a ferromagnetic (F) layer sandwiched between an insulating (I) layer and a nonmagnetic heavy metal (NM) layer with strong spin-orbit coupling. The NM, F, and I layers are all uniformly thick. The stable states of magnetization are illustrated with black and white arrows along the $+z$- and $-z$-directions. The magnetic energy landscape is shaped with respect to the current flow (spin accumulation) to ensure that a current pulse of appropriate amplitude and duration favors a specific stable state of magnetization, thereby allowing $\mathbf{T}_{\mathrm{DL}}$ to deterministically switch the perpendicular magnetization without the need for a magnetic field.

The ALPE device, shown in Fig. 1(a) and (b), possesses a perpendicular magnetic anisotropy (PMA) originating from the

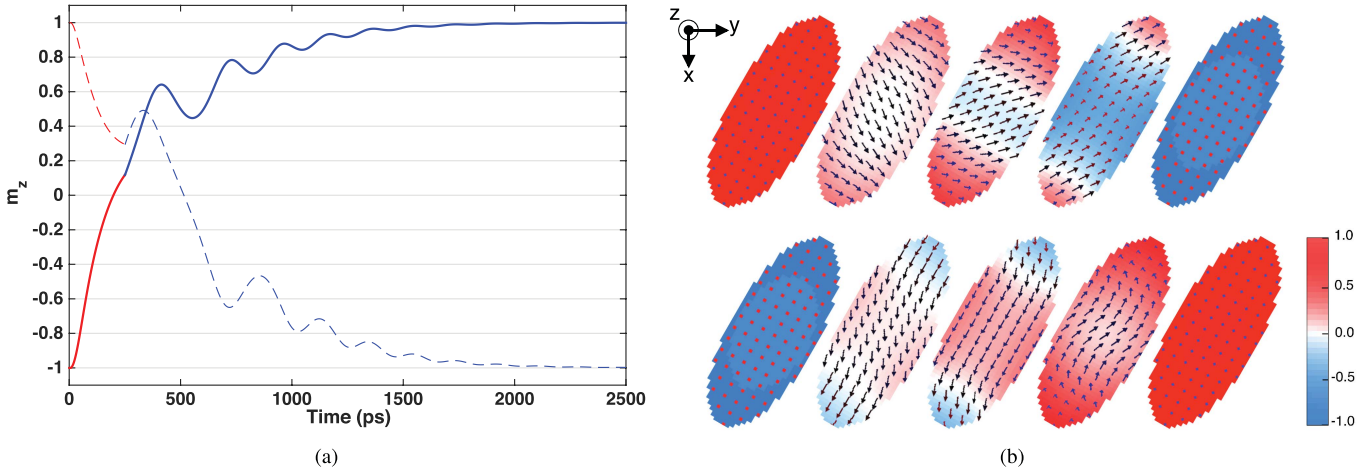

(a) (b)

Fig. 2. All-spin-orbit toggle switching of the perpendicular magnetization. (a) Current pulse with a duration of 250 ps providing a density of 4.5×10^8 A/cm^2 switches the magnetization independent of the IS ($+z$ or $-z$). $\mathbf{m}_z$ indicates the normalized magnetization in the perpendicular-to-the-plane [001] direction. (b) Magnetization vector diagrams at (from the left to the right) $t = 0$, 250 ps, 500 ps, 1 ns, and 2.5 ns, respectively, exhibiting switching operation from the $+z$-direction to the $-z$-direction (top) and from the $-z$-direction to the $+z$-direction (bottom). Color bar indicates the normalized magnetization in the perpendicular-to-the-plane [001] direction ($\mathbf{m}_z$).

interface of the *NM* and *F* layers, an interfacial system widely utilized to achieve strong PMA [4], [5]. The cross section of the $F|I$ pillar, shown in Fig. 1(b), is elliptical. Hence, the magnetic energy landscape of the device, shown in Fig. 1(c), is shaped to ensure that certain energy contours cross the plane of the device ($x - y$ plane). The length of the $F|I$ pillar encloses an angle of Θ degrees with the current flow (y-axis). Consequently, the axis of the x–y crossing energy contours is misaligned with respect to the spin accumulation direction (x-axis) by an angle of Θ, which, as discussed later, is chosen to achieve deterministic switching in both toggle and nontoggle modes, offering significant design flexibility to memory and logic systems.

III. Operation of the ALPE Device

By injecting an in-plane current pulse into the *NM* layer, as shown in Fig. 1(a), the coupling between the electron spin and orbital motion leads to nonequilibrium spin accumulation, exerting SOTs on the magnetization. As the spin accumulation acts through the perpendicular area (A) of the $F|I$ pillar and the injected charge current flows through the in-plane area (a) of the *NM* layer, the spin-to-charge current ratio is proportional to A/a which is much larger than one. Hence, for an electron charge flowing through the *NM* layer, many $\hbar/2$ units of angular momentum flow perpendicular to the $F|I$ pillar, applying SOTs to the device magnetization. Since the field-like torque $\mathbf{T}_{\mathrm{FL}}$ can be negligible in comparison with the damping-like torque $\mathbf{T}_{\mathrm{DL}}$ [5], the auxiliary effect of $\mathbf{T}_{\mathrm{FL}}$ on device behavior is ignored. As shown in Fig. 1(d), $\mathbf{T}_{\mathrm{DL}}$ moves the magnetization direction from the perpendicular stable state [initial state (IS)] along the z-axis toward the $x-y$ plane. Once the magnetization direction is sufficiently far from the z-axis, the current pulse is turned off [pulse-OFF state (PS)], $\mathbf{T}_{\mathrm{DL}}$ vanishes, and the magnetization crosses the $x - y$ plane by precessing along the x–y crossing energy contours. The magnetization relaxes along the other perpendicular stable state [final state (FS)] by precessing and dissipating energy through damping.

TABLE I
ALPE Device Parameters

Parameter	Numerical value †	Description
t_F	1.5×10^{-7} cm	F layer thickness
w_F	60×10^{-7} cm^3	F layer width
l_F	150×10^{-7} cm^3	F layer length
l	150×10^{-7} cm	Channel length
w	100×10^{-7} cm	Channel width
d	2×10^{-7} cm	Channel thickness
M_{s_0}	1.2×10^3 emu/cm^3	Saturation mag.
K_{u_0}	9.407×10^6 erg/cm^3	Magnetic anisotropy
ρ_c	15×10^{-6} Ωcm	Channel resistivity [7]
α	0.1	Damping factor [4]-[7]
β	8.3×10^{-4} K^{-1}	Variation rate of M_s
η	2.2×10^{-3} K^{-1}	Variation rate of K_u
k_B	1.38×10^{-16} erg/K	Boltzmann constant
e	1.6×10^{-19} C	Charge quantum
$\hbar$	1.05×10^{-27} ergs	Planck constant
Θ	$\pi/3$	Tilt angle
$\mathbf{T}_{\mathrm{DL}}^0$	$\zeta_{\mathrm{DL}} \frac{\hbar}{2\mathrm{eMst}_F}\mathbf{J}$	Torque prefactor
ζ_{DL}	0.12	Torque coefficient [12]*

† Numerical values at 300 K

* ζ_{DL} represents the efficiency of $\mathbf{J}$ in producing a damping-like torque.

For a tilt angle $\Theta = 0°$, the magnetic energy landscape is symmetric with respect to the current flow. Therefore, independent of the IS of the magnetization ($+z$- or $-z$-direction), the FS of the magnetization is relaxed to either the identical or reverse direction with respect to the IS, depending upon the amplitude and duration of the injected current pulse. The device, therefore, behaves in the toggle mode of switching, where a current pulse with an appropriate amplitude and duration can switch the magnetization from the $+z$- to $-z$-direction and vice versa. For longer pulse durations or larger pulse amplitudes, $\mathbf{T}_{\mathrm{DL}}$ moves the magnetization closer

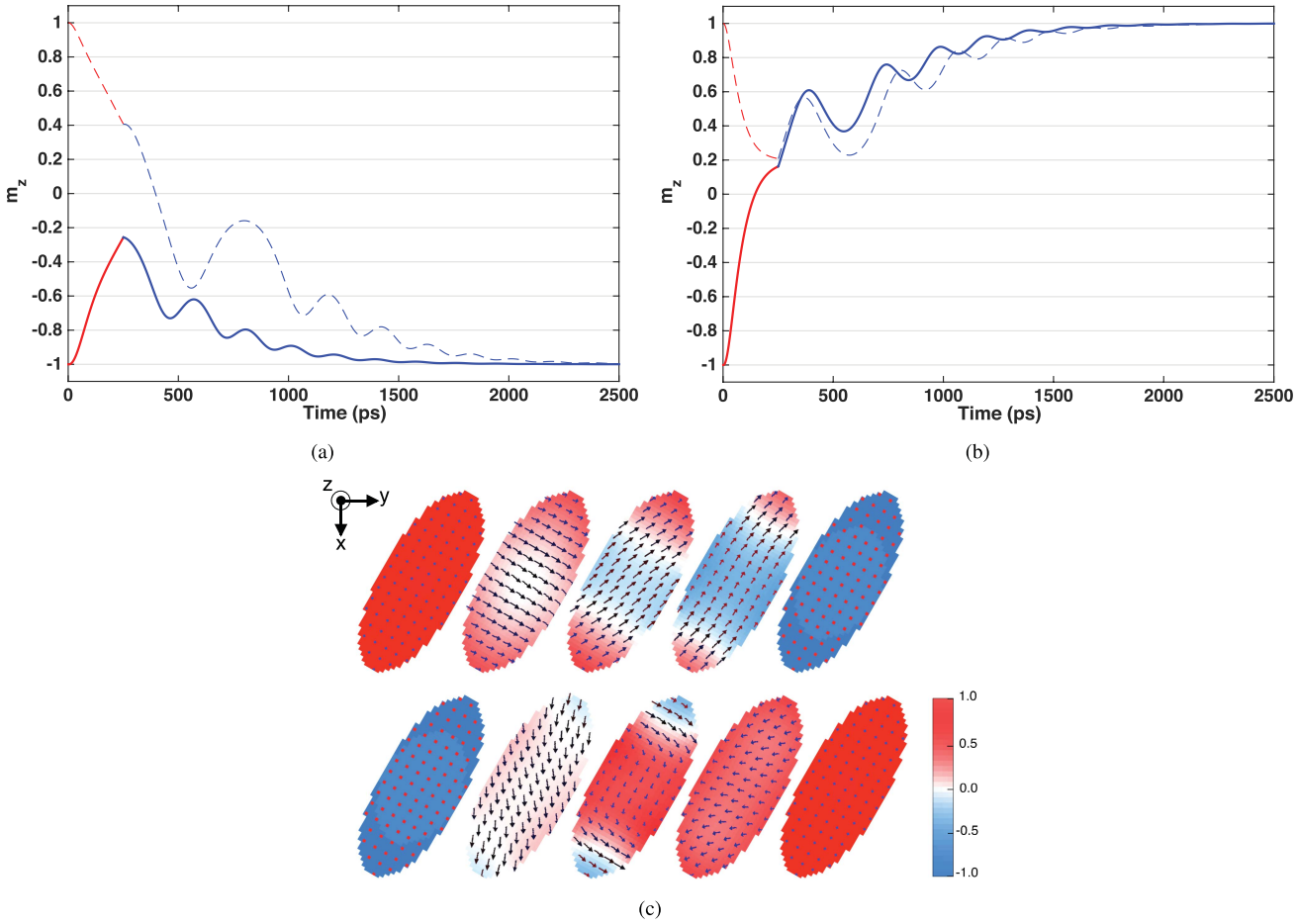

Fig. 3. All-spin-orbit nontoggle switching of the perpendicular magnetization. The energy landscape of the device with a nonzero tilt angle Θ ($= \pi/3$) is asymmetric with respect to the current flow and thereby with respect to $\mathbf{T}_{\mathrm{DL}}$. The device can, therefore, be switched in both toggle and nontoggle modes. (a) Current pulse with a duration of 250 ps providing a density of 3×10^8 A/cm^2 switches the magnetization from the $+z$- to $-z$-direction but not from the $-z$- to $+z$-direction. (b) Current pulse with a duration of 250 ps providing a density of 6×10^8 A/cm^2 switches the magnetization from the $-z$- to $+z$-direction but not from the $+z$- to $-z$-direction. (c) Magnetization vector diagrams at (from the left to the right) $t = 0$, 250 ps, 500 ps, 1 ns, and 2.5 ns, respectively, exhibiting switching operation from the $+z$-direction to the $-z$-direction (top) and from the $-z$-direction to the $+z$-direction (bottom).

to the metastable state along the spin accumulation orientation (x-axis). Consequently, longer pulse durations or larger pulse amplitudes are more susceptible to thermal magnetization fluctuations.

By applying an azimuthal rotation of Θ to the $F|I$ pillar [Fig. 1(b)], which is achieved by conventional lithography, the axis of the x–y crossing energy contours is misaligned with respect to the x-axis by an angle of Θ [Fig. 1(c)]. Hence, although pulses with sufficiently long durations or large amplitudes align the magnetization with the x-axis, the magnetization deterministically precesses along the x–y crossing energy contours, once the current pulse is turned off. Furthermore, a nonzero Θ breaks the symmetry of the magnetic energy landscape with respect to the current flow and $\mathbf{T}_{\mathrm{DL}}$. The device can consequently behave in the nontoggle mode, where, depending on the IS of the magnetization, pulses with different amplitudes are required to switch the magnetization, and the toggle mode, where a pulse with an appropriate amplitude can switch the magnetization independent of the IS.

The macrospin and micromagnetic simulations of the ALPE device are performed by choosing Pt, Co, and AlO_x, as, respectively, the *NM*, *F*, and *I* layers. Magnetization trajectories are determined based on a modified Landau–Lifshitz–Gilbert–Slonczewski (LLGS) [19] equation, which considers the effect of temperature on the device behavior (for details, see the Appendix). Magnetization vector diagrams are determined by finite element micromagnetic simulations using object oriented micromagnetic framework [20]. The device parameters are listed in Table I.

Magnetization trajectories and vector diagrams for different amplitudes of a current pulse with a duration of 250 ps, injected into the Pt|Co|AlO_x device, are shown in Figs. 2 and 3. A trajectory from the IS to the FS is segmented into two lines. The red (blue) line illustrates the trajectory during the pulse injection (relaxation after the pulse injection). The effect of the temperature is initially omitted ($T = 0$ K) and discussed later in this paper.

As shown in Fig. 2, a current pulse producing a 4.5×10^8 A/cm^2 current density switches the magnetization

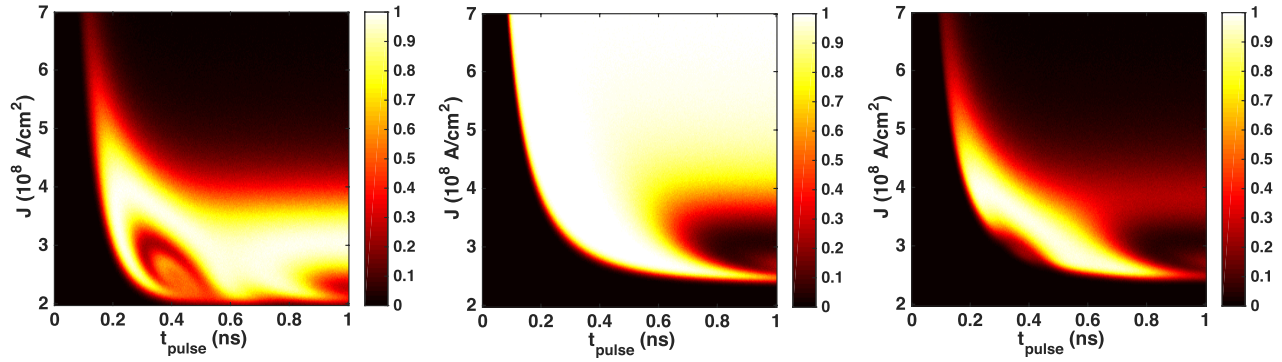

Fig. 4. Switching probability as a function of pulse duration t_{pulse} and pulse amplitude (current density). (a) Switching events from the $+z$- to $-z$-direction for the device with a tilt angle $\Theta = 60°$. (b) Switching events from the $-z$- to $+z$-direction for the device with a tilt angle $\Theta = 60°$. (c) Toggle switching events for the device with a tilt angle $\Theta = 60°$. The calculations were repeated 1,000 times for each pixel; the white (black) region represents high (low) switching probability.

by 180° independent of the IS of the magnetization ($+z$- or $-z$-direction). Alternatively, as shown in Fig. 3, a pulse producing 3×10^8 A/cm^2 (6×10^8 A/cm^2) can only switch the magnetization if the IS is along the $+z$ ($-z$)-direction. The device, therefore, operates in both toggle and nontoggle modes of switching, achievable by setting the amplitude of the injected current pulse.

The direction of the current injected into the device ($+y$ or $-y$) does not affect the switching process. Although changing the sign of the current pulse reverses the sign of the spin accumulation polarization, the magnetization experiences the same magnetic energy landscape. As demonstrated in Fig. 1(b) and (c), the magnetic energy landscape of the device is symmetric with respect to the axis which makes an angle of Θ with the current flow along the y-axis. Hence, the switching operation of the device is controlled by the amplitude and duration of the injected current pulse, and is independent of the polarity of the current pulse.

Injecting a current pulse increases the device temperature through the Joule heating effect, thereby decreasing the magnetic anisotropy and saturation magnetization [5], [7], [8]. Furthermore, the nonzero temperature introduces thermal magnetization fluctuations [21]. Considering the Joule heating effect and thermal magnetization fluctuations, the switching probability as a function of the current pulse duration and amplitude are shown in Fig. 4. Device parameters are listed in Table I. For switching events from the $+z$- to $-z$-direction, deterministic switching is observed for a wide range of current pulse durations within the low current density regime, as shown in Fig. 4(a). For switching events from the $-z$- to $+z$-direction, deterministic switching is observed for a wide range of current densities within the short pulse regime as shown in Fig. 4(b). Product of the switching probability diagrams in Fig. 4(a) and (b) is shown in Fig. 4(c), illustrating high switching probability in the short pulse and low current regime for toggle switching events. Consequently, ultrahigh speed and energy-efficient switching at both toggle and nontoggle modes is achieved by choosing the appropriate current pulse duration and amplitude.

The energy dissipated by the device during a switching operation is due to ohmic loss from current injection.

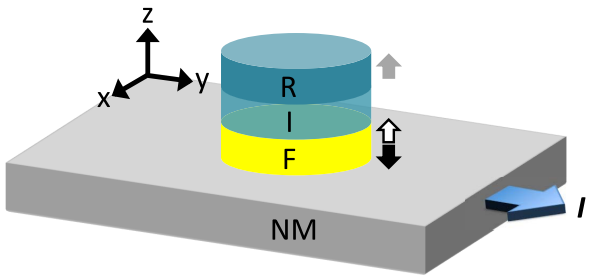

(a)

Fig. 5. All-spin-orbit perpendicular-anisotropy MTJ.

The estimated energy, consumed by a device with a channel resistivity of 15 $\mu\Omega$cm and a channel length, width, and thickness of, respectively, 150, 100, and 2 nm, is approximately 23 fJ. The ALPE device enhances the switching energy-time product by two orders of magnitude as compared with the optimized state-of-the-art perpendicularly magnetized devices switched by spin-transfer torques [22].

As demonstrated in Fig. 5, the magnetic state of the device can be read through the tunneling magnetoresistance effect, by integrating a magnetic reference (R) layer on top of the device, forming a three terminal magnetic tunnel junction (MTJ). The resistance of the MTJ is low (high), if the magnetization of the F layer is parallel (antiparallel) to the magnetization of the R layer, permitting the magnetic state of the device to be read.

IV. Conclusion

A device with perpendicular magnetization is presented, which can be deterministically switched utilizing current-induced SOTs without the need for any magnetic field. The magnetic energy landscape is demonstrated to be the key to all-spin-orbit switching of perpendicular magnetization. The device is deterministically switched in both toggle and nontoggle modes by choosing the amplitude or duration of the injected current pulse. The device enhances the switching energy-time product by two orders of magnitude as compared with state-of-the-art perpendicularly magnetized devices switched by spin-transfer torques.

APPENDIX

In this section, a model for the ALPE device is described, which considers the effect of Joule heating and temperature on device behavior. The magnetic dynamics of the device under the effect of the SOTs at room temperature is described by the temporal evolution of the magnetization governed by the LLGS [19] equation,

$$\frac{d\mathbf{m}}{dt} = -\gamma\,\mathbf{m} \times \mathbf{H}_{\text{eff}} + \alpha\mathbf{m} \times \frac{d\mathbf{m}}{dt} + \gamma\,\mathbf{T}_{\text{DL}}, \tag{1}$$

where $\mathbf{m} = (m_x, m_y, m_z)$ is a unit vector along the magnetization, which at any instant of time, makes an angle ϑ with $\hat{z}$, while the plane of $\mathbf{m}$ and $\hat{z}$ makes an angle φ with $\hat{x}$. α is the Gilbert damping factor causing relaxation of the magnetization to the equilibrium orientation, and $\gamma = g\mu_B/\hbar$ is the gyromagnetic ratio, where μ_B is the Bohr magneton and g is the g-factor. $\mathbf{T}_{\text{DL}} = (\hbar/2e)(\mathbf{J}(t)/M_s t_F)\zeta_{\text{DL}}\ \mathbf{m} \times (\boldsymbol{x} \times \mathbf{m})$ denote the damping-like SOT [5]. M_s and t_F denote the saturation magnetization and thickness of the ferromagnetic layer and ζ_{DL}, equivalent to the spin Hall angle in the literature [5], [8], [12], [15], represents the efficiency of the charge current density $\mathbf{J}(t)$ in producing $\mathbf{T}_{\text{DL}}$. $\mathbf{H}_{\text{eff}}$, the effective field experienced by magnetization, is

$$\mathbf{H}_{\text{eff}} = \mathbf{H}_k(\mathbf{m}) + \mathbf{H}_d(\mathbf{m}) + \mathbf{H}_L \tag{2}$$

$\mathbf{H}_k(\mathbf{m})$ denotes the perpendicular-to-the-plane magnetic anisotropy field

$$\mathbf{H}_k(\mathbf{m}) = 2\frac{K_u}{M_s}(\mathbf{m}.\hat{z})\hat{z} \tag{3}$$

where K_u and M_s are, respectively, the magnetic anisotropy and saturation magnetization. $\mathbf{H}_d(\mathbf{m})$ denotes the demagnetization field

$$\begin{aligned}\mathbf{H_d}(\mathbf{m}) = &-4\pi M_s(N_i \sin(\vartheta)\sin(\varphi - \Theta)\hat{i} \\ &+ N_j \sin(\vartheta)\cos(\varphi - \Theta)\hat{j} \\ &+ N_z \cos(\vartheta)\hat{z})\end{aligned} \tag{4}$$

where N_i, N_j, and N_z are the demagnetizing factors and $N_i + N_j + N_z = 1$. Here, $\hat{i} = -\sin(\Theta)\hat{x} + \cos(\Theta)\hat{y}$ and $\hat{j} = \cos(\Theta)\hat{x} + \sin(\Theta)\hat{y}$ represent the unit vectors along, respectively, the length and width of the $F|I$ pillar. Θ denotes the tilt angle enclosed by the length of the $F|I$ pillar ($\hat{i}$) and current flow ($\hat{y}$). Variations in the target device size and Θ exhibit a small effect on the demagnetization factors, N_i, N_j, and N_z. Hence, variations in the target size and Θ do not have a detectable effect on the device performance, particularly when thermal fluctuations are considered. The effect of thermal fluctuations is several orders of magnitude greater than the effect of variations for the target device size and Θ.

A nonzero temperature introduces thermal fluctuations to the magnetization which is modeled by the Langevin random field $\mathbf{H}_L = (H_{L,x}, H_{L,y}, H_{L,z})$. Each component of $\mathbf{H}_L$ follows a zero-mean Gaussian random process, whose standard deviation is a function of temperature [21],

$$\delta = \sqrt{\frac{2\alpha k_B T}{\gamma\, M_s v_F\, \Delta t}} \tag{5}$$

where α is the Gilbert damping factor, γ is the gyromagnetic ratio, k_B is the Boltzman constant, M_s is the saturation magnetization, v_F is the ferromagnetic layer volume, T denotes the temperature, and Δt is the duration of the constant effective thermal fluctuation field. As the current flows into the device, the temperature increases through the Joule heating effect, proportional to the square of the current [7], [8]

$$T(I) = T_0 + kI^2 \tag{6}$$

where I is the amplitude of the current, T_0 is the temperature at zero current, and k relates the temperature variations to the Joule heating. The effective field $\mathbf{H}_{\text{eff}}$ may change due to variations in device parameters caused by Joule heating [5], [7], [8]. Specifically, injecting a current pulse into a perpendicularly magnetized $NM|F|I$ heterostructure reduces the saturation magnetization and magnetic anisotropy of the device through Joule heating. The Joule heating effect is, therefore, accurately considered. Since a small amount of current is injected into the device over a short period of time, most of the Joule heating related terms are negligible [5], [7], [8], and those terms that linearly vary as a function of temperature are significant

$$M_s(T) = M_{s0}(1 - \beta(T - T_0)) \tag{7}$$

$$K_u(T) = K_{u0}(1 - \eta(T - T_0)) \tag{8}$$

where M_{s0} and K_{u0} are, respectively, the saturation magnetization and magnetic anisotropy at temperature T_0. Coefficients β and η represent the change in, respectively, M_s and K_u when the temperature changes by $T - T_0$. Substituting (6) in (7) and (8), the saturation magnetization and magnetic anisotropy are proportional to the square of the current amplitude as, respectively, as

$$M_s(T) = M_{s0}(1 - \beta k I^2) \tag{9}$$

$$K_u(T) = K_{u0}(1 - \eta k I^2). \tag{10}$$

These equations explicitly exhibit the variation of each parameter caused by Joule heating.

REFERENCES

[1] S. Zhang, P. M. Levy, and A. Fert, "Mechanisms of spin-polarized current-driven magnetization switching," *Phys. Rev. Lett.*, vol. 88, p. 236601, May 2002.

[2] Y. Tserkovnyak, A. Brataas, and G. E. W. Bauer, "Theory of current-driven magnetization dynamics in inhomogeneous ferromagnets," *J. Magn. Magn. Mater.*, vol. 320, pp. 1282–1292, Apr. 2008.

[3] I. M. Miron *et al.*, "Current-driven spin torque induced by the Rashba effect in a ferromagnetic metal layer," *Nature Mater.*, vol. 9, pp. 230–234, Jan. 2010.

[4] I. M. Miron *et al.*, "Perpendicular switching of a single ferromagnetic layer induced by in-plane current injection," *Nature*, vol. 476, no. 7359, pp. 189–193, Aug. 2011.

[5] L. Liu, O. J. Lee, T. J. Gudmundsen, D. C. Ralph, and R. A. Buhrman, "Current-induced switching of perpendicularly magnetized magnetic layers using spin torque from the spin Hall effect," *Phys. Rev. Lett.*, vol. 109, p. 096602, Aug. 2012.

[6] O. C. Avci *et al.*, "Magnetization switching of an MgO/Co/Pt layer by in-plane current injection," *Appl. Phys. Lett.*, vol. 100, p. 212404, May 2012.

[7] K. Garello *et al.*, "Symmetry and magnitude of spin-orbit torques in ferromagnetic heterostructures," *Nature Nanotechnol.*, vol. 8, pp. 587–593, Jul. 2013.

[8] J. Kim *et al.*, "Layer thickness dependence of the current-induced effective field vector in Ta|CoFeB|MgO," *Nature Mater.*, vol. 12, pp. 240–245, Dec. 2012.
[9] T. Suzuki *et al.*, "Current-induced effective field in perpendicularly magnetized Ta/CoFeB/MgO wire," *Appl. Phys. Lett.*, vol. 98, no. 14, p. 142505, Apr. 2011.
[10] X. Fan *et al.*, "Observation of the nonlocal spin-orbital effective field," *Nature Commun.*, vol. 4, p. 1799, Apr. 2013.
[11] O. J. Lee *et al.*, "Central role of domain wall depinning for perpendicular magnetization switching driven by spin torque from the spin Hall effect," *Phys. Rev. Lett.*, vol. 89, pp. 0244181–0244188, Jan. 2014.
[12] W. Zhang, W. Han, X. Jiang, S.-H. Yang, and S. S. P. Parkin, "Role of transparency of platinum–ferromagnet interfaces in determining the intrinsic magnitude of the spin Hall effect," *Nature Phys.*, vol. 11, pp. 496–502, Apr. 2015.
[13] C.-F. Pai, L. Liu, Y. Li, H. W. Tseng, D. C. Ralph, and R. A. Buhrman, "Spin transfer torque devices utilizing the giant spin Hall effect of tungsten," *Appl. Phys. Lett.*, vol. 101, no. 12, p. 122404, Sep. 2012.
[14] M. Kazemi, G. E. Rowlands, E. Ipek, R. A. Buhrman, and E. G. Friedman, "Compact model for spin–orbit magnetic tunnel junctions," *IEEE Trans. Electron Devices*, vol. 63, no. 2, pp. 848–855, Feb. 2016.
[15] L. Liu, C.-F. Pai, Y. Li, H. W. Tseng, D. C. Ralph, and R. A. Buhrman, "Spin-torque switching with the giant spin Hall effect of tantalum," *Science*, vol. 336, no. 6081, pp. 555–558, May 2012.
[16] S. Mangin, D. Ravelosona, J. A. Katine, M. J. Carey, B. D. Terris, and E. E. Fullerton, "Current-induced magnetization reversal in nanopillars with perpendicular anisotropy," *Nature Mater.*, vol. 5, no. 3, pp. 210–215, Feb. 2006.
[17] G. Yu *et al.*, "Switching of perpendicular magnetization by spin–orbit torques in the absence of external magnetic fields," *Nature Nanotechnol.*, vol. 9, pp. 548–554, May 2014.
[18] Y. Long *et al.*, "Switching of perpendicularly polarized nanomagnets with spin orbit torque without an external magnetic field by engineering a tilted anisotropy," *Proc. Nat. Acad. Sci. USA*, vol. 112, pp. 10310–10315, Aug. 2015.
[19] J. C. Slonczewski, "Current-driven excitation of magnetic multilayers," *J. Magn. Magn. Mater.*, vol. 159, pp. L1–L7, Jun. 1996.
[20] M. J. Donahue and D. G. Porter, "OOMMF user's guide," NIST, Gaithersburg, MD, USA, Interagency Rep. NIST IR 6376, Sep. 1999.
[21] W. F. Brown, Jr., "Thermal fluctuations of a single-domain particle," *Phys. Rev.*, vol. 130, no. 5, pp. 1677–1686, Jun. 1963.
[22] K. Ikegami *et al.*, "Low power and high density STT-MRAM for embedded cache memory using advanced perpendicular MTJ integrations and asymmetric compensation techniques," in *Proc. IEEE Int. Electron Devices Meeting*, Dec. 2014, pp. S28.1.1–S28.1.4.

Authors' photographs and biographies not available at the time of publication.